DOE/ET-53088-331 IFSR#331

Nonlinear Growth of the Quasi-Interchange Instability

F.L. Waelbroeck
Institute for Fusion Studies
The University of Texas at Austin
Austin, Texas 78712

July 1988

Nonlinear Growth of the Quasi-Interchange Instability

F.L. Waelbroeck
Institute for Fusion Studies
The University of Texas at Austin
Austin, Texas 78712

Abstract

The nonlinear growth of the low-shear quasi-interchange instability is investigated using a low-beta expansion of the Reduced Magnetohydrodynamic equations. These equations are shown to be identical to the full Magnetohydrodynamic equations in the linear regime except for the neglect of parallel kinetic energy and the effects of compressibility. The nonlinear forces are found to be stabilizing for the profiles investigated. These forces lead to the appearance of stable, finite amplitude bifurcated equilibria above marginal stability.

I. Introduction

Ideal magnetohydrodynamic instabilities are often invoked to explain rapid, large-scale instabilities in magnetic confinement experiments. However, in view of the relatively slow evolution of the equilibrium, it is not clear how such instabilities can appear suddenly as fast growing modes. This problem has received renewed attention as a result of the observation of extremely fast sawtooth crashes with no precursor oscillations.[1]

In this paper nonlinear effects on the growth of a pressure-driven, interchange-like mode are investigated. This mode is thought to be responsible for the sawtooth crashes observed in JET and successfully accounts for most of their features.[2–6] The analysis presented here differs from previous bifurcation calculations[7,8] by the inclusion of toroidal coupling effects. Toroidal curvature, which is important for pressure-driven modes, destroys the helical symmetry which is typical of kink-like instabilities.

The nonlinear corrections are evaluated by expanding the equations of motion for the unstable mode near marginal stability.[7] This procedure yields the following equation for the mode amplitude ξ:

$$\frac{d^2\xi}{dt^2} = \gamma^2\xi + \Gamma\xi^3 + O(\xi^5) , \tag{1}$$

where γ is the linear growth rate. The coefficient Γ is the main goal of the analysis. Its sign determines the qualitative behavior of the mode as the linear stability threshold is crossed:

(1) For $\Gamma < 0$, the nonlinear terms are stabilizing and lead to the appearance of secondary, stable equilibria. In this case the plasma will simply shift adiabatically from the initial unstable equilibrium branch to the nearby bifurcated equilibrium branch (Fig. 1a).

(2) For $\Gamma > 0$, however, there are no nearby equilibria above marginal stability (Fig. 1b). A robust, explosive instability can develop even near the stability threshold. In the absence of higher-order stabilizing terms the mode would grow to infinite amplitude over a finite time.

These two cases are referred to as supercritical and subcritical bifurcations, respectively.

The analysis is developed from the high-beta reduced magnetohydrodynamic (RMHD) equations of Strauss.[9] These equations describe nonlinear plasma dynamics in large aspect ratio tokamak geometry. They are the result of a systematic ordering of the magnetohydrodynamic (MHD) equations, in which only the lowest order terms in the inverse aspect ratio, $\varepsilon = a/R_0$, are retained (here a is the minor radius and R_0 the major radius of the torus). In particular, RMHD takes $\beta \sim k_{\|} \sim \varepsilon$, where $\beta = P/B_0^2$ is the ratio of kinetic pressure to magnetic pressure and $k_{\|} = B^{-1}(\mathbf{B} \cdot \boldsymbol{\nabla})$ is the inverse of the characteristic scale length along the magnetic field.

In order to describe interchange-like instabilities in relatively low-beta plasmas, we introduce the secondary ordering parameter δ and assume $\beta \sim k_{\|} \sim \varepsilon\delta$, with $\delta \ll 1$. Note that a global instability with $k_{\|} \ll \varepsilon$ can only occur if the plasma contains a low-shear resonant region where the safety factor q is close to a rational number: specifically, $q - q_s \sim \delta$ where $q_s = m/n$. The quasi-interchange model of sawtooth disruptions assumes that this condition holds in a central region of the plasma with $q_s = 1$.

The basic nonlinear interchange equations are then derived by expanding the RMHD equations to lowest significant order in δ. However, consistency with the reduced MHD ordering requires $\varepsilon \ll \delta$. This condition is generally not satisfied, typical values of the inverse aspect ratio being $\varepsilon \sim 1/4$. Nonetheless, one would expect RMHD to remain qualitatively valid, particularly for pressure-driven modes, when $\delta \lesssim \varepsilon$. This hypothesis is supported by an examination of the linearized MHD equation in the low-shear, low-beta approximation.[10,6]

The exact (non-reduced) energy principle for these equations contains the following terms:

(i) Cylindrical kink and line-bending terms proportional to $(q - q_s)^2$.

(ii) Interchange terms proportional to $(p')^2$, including the sideband energy.

(iii) A term proportional to $p'(q^2 - 1)$.

The first two terms are clearly included in the RMHD equations, but the last term will be missing. For $q_s = 1$, however, this term should be neglected from the MHD equations as well. This is of course the case relevant to the sawtooth problem, and we thus conclude that the RMHD equations will produce the correct potential energy for the quasi-interchange in this case.

The RMHD kinetic energy, however, neglects the parallel velocity and the effects of compressibility. Compressibility is unimportant near marginal stability, while the neglect of parallel velocity will result in growth rates being overestimated by a factor of $(1+2q_s^2)^{1/2}$. This clearly does not affect the nature of the bifurcation.

The RMHD equations are described in Sec. II. The interchange ordering, $\delta \ll 1$, is used in Sec. III to simplify the system further. The resulting, "interchange-reduced" equations involve only the helically resonant components of the fields, but contain numerical constants related to the behavior of the non-resonant components in the sheared outer region of the plasma. The perturbation expansion in the mode amplitude is described in Sec. IV and the resulting equations are solved for model profiles in Sec. V. The results are discussed in Sec. VI.

II. Formulation

The RMHD system is derived in detail in the paper by Strauss[9] and is presented here mainly for ease of reference.

The coordinate system is defined in terms of cylindrical coordinates (R, ζ, Z) by $x = (R-R_0)/a$, $y = Z/a$ and $z = -\zeta$, where x and y are coordinates in the poloidal plane and z is the toroidal angle. The magnetic field is given in sufficient accuracy by

$$\mathbf{B} = \hat{z} + \varepsilon(-\hat{z}x + \hat{z}B_{\|} - \hat{z} \times \boldsymbol{\nabla}_{\perp}\psi) , \tag{2}$$

where ψ is the poloidal flux and $B_{\|}$ represents diamagnetic corrections to the vacuum toroidal field. All operations involving the perpendicular gradient operator

$$\boldsymbol{\nabla}_\perp = \hat{x}\,\frac{\partial}{\partial x} + \hat{y}\,\frac{\partial}{\partial y} , \tag{3}$$

are to be carried out using the Euclidean metric. The lowest order force balance equation,

$$\boldsymbol{\nabla}_\perp (B_{||} + p/2) = 0 , \tag{4}$$

allows $B_{||}$ to be eliminated in favor of the pressure p. An important operator for interchange-like modes is the parallel gradient operator,

$$\mathbf{B} \cdot \boldsymbol{\nabla} = \varepsilon \nabla_{||} . \tag{5}$$

This operator is conveniently expressed in terms of the conventional bracket,

$$[f, g] \quad = \quad \hat{z} \cdot (\boldsymbol{\nabla}_\perp f \times \boldsymbol{\nabla}_\perp g) , \tag{6}$$

by

$$\nabla_{||} \quad = \quad \frac{\partial}{\partial z} - [\psi, \cdot] . \tag{7}$$

Ampere's law is written

$$J = \boldsymbol{\nabla}_\perp^2 \psi , \tag{8}$$

where J is the negative of the toroidal current density.

The principal dynamical equation is the shear-Alfvén law, given by

$$\frac{\partial U}{\partial \tau} + [\varphi, U] = -\nabla_{||} J - [x, p] , \tag{9}$$

where the vorticity U is given in terms of the stream function φ by

$$U = \boldsymbol{\nabla}_\perp^2 \varphi . \tag{10}$$

The left-hand-side of the shear-Alfvén law contains the convective derivative of the vorticity while the right-hand side consists of the parallel-current driving term and the interchange term. The system is completed by the parallel Ohm's law,

$$\frac{\partial \psi}{\partial \tau} + \nabla_{\parallel} \varphi = 0 \ , \tag{11}$$

and the pressure evolution equation,

$$\frac{\partial p}{\partial \tau} + [\varphi, p] = 0 \ . \tag{12}$$

The analysis of these equations is simplified by making use of such properties of the bracket as antisymmetry and the Jacobi identity:

$$[f, g] = -[g, f] \ , \tag{13}$$

$$[f, [g, h]] + [g, [h, f]] + [h, [f, g]] = 0 \ . \tag{14}$$

It should also be noted that the bracket is a derivation: it satisfies

$$[f, gh] = [f, g] \cdot h + [f, h] \cdot g \ . \tag{15}$$

The integral invariants of RMHD can also be used to reduce the complexity of the problem. These can be derived from the identities[11]

$$\int f[g, h] dV = \int g[h, f] dV = \int h[f, g] dV \ , \tag{16}$$

which can be seen to hold by writing the bracket as a divergence,

$$[f, g] = \boldsymbol{\nabla}_{\perp} \cdot (g \hat{z} \times \boldsymbol{\nabla}_{\perp} f) \ , \tag{17}$$

and integrating by parts, assuming the vanishing of surface terms. The following integral invariants are particularly useful:

$$C = \int F(p) dV \ , \tag{18}$$

$$D = \int G(\nabla_{\parallel} p) dV \ , \tag{19}$$

where F and G are arbitrary functions.

In the following analysis we will consider only conditions such that the pressure is initially a flux function: $\nabla_{||}p = 0$ at $\tau = 0$. Equation (19) then implies

$$\nabla_{||} p = 0 \tag{20}$$

at all possible times ($\tau > 0$).

To summarize, the RMHD system consists of Eqs. (9), (11), and (12), with the defining relations (8) and (10). Equation (12) will be replaced by Eq. (20) under the assumption stated above.

III. Interchange-Reduced Equations

A. Simplification of the equations

The quasi-interchange ordering allows considerable simplification of the equations of motion. The simplification is largely a consequence of the partial linearization resulting from the small-δ expansion. It is important to note, however, that no assumptions regarding the size of the perturbation from equilibrium are made. In this sense, the interchange-reduced equations remain fully nonlinear.

The analysis in this subsection follows a similar derivation by Kotschenreuther et al.[12]

In terms of the normalized variables used in RMHD the quasi-interchange ordering becomes simply $p \sim \nabla_{||} \sim \delta \ll 1$, the ϵ terms being absorbed in the normalization. The equations of motion then imply $\frac{\partial}{\partial \tau} \sim \delta$. To zeroth order the plasma is thus in a force-free, closed-line, cylindrically symmetric equilibrium. Clearly this state is marginally stable to the exchange of flux tubes. Introducing polar coordinates in the poloidal plane by $x = r\cos\theta$

and $y = r\sin\theta$, we obtain the resonance condition on interchange perturbations ξ as

$$\nabla_{\|}\xi = \frac{\partial\xi}{\partial\theta} + \frac{\partial\xi}{\partial\zeta} = 0 \; . \tag{21}$$

It is satisfied by $\xi = f(r, \theta - \zeta)$, for arbitrary f. Thus, the quasi-interchange ordering describes the evolution of the plasma between states which are, to lowest order, helically symmetric. This observation motivates the change of coordinates $(r, \theta, \zeta) \to (r, \alpha, \eta)$, where $\alpha = \theta - \zeta$ and $\eta = \zeta$. α is a field-line label for the zeroth-order magnetic field. The bracket in these new coordinates is simply

$$[f, g] = \frac{1}{r}\left\{\frac{\partial f}{\partial r}\frac{\partial g}{\partial \alpha} - \frac{\partial f}{\partial \alpha}\frac{\partial g}{\partial r}\right\} \; . \tag{22}$$

The parallel gradient is then most simply expressed in terms of the helical flux defined by

$$\chi \;=\; \psi + r^2/2 \; . \tag{23}$$

We then have

$$\nabla_{\|} \;=\; \frac{\partial}{\partial\eta} - [\chi, \cdot] \; . \tag{24}$$

Note that $\chi \sim \delta$.

The dynamics of interchange perturbations are of course determined by higher-order terms. For finite δ, the helical symmetry is broken by the toroidal curvature. Nonetheless, the field quantities remain approximately helically symmetric. It is useful to separate them into their η-averaged part,

$$\overline{F} \;=\; \frac{1}{2\pi}\oint d\eta\; f(r, \alpha, \eta) \; , \tag{25}$$

and an η-fluctuating remainder,

$$\tilde{f} \;=\; f - \overline{F} \; . \tag{26}$$

$\overline{F}$ clearly satisfies the resonance condition, Eq. (21). Note that the bracket behaves as a typical quadratic form under helical averaging:

$$\overline{[f,g]} = [\overline{F},\overline{g}] + \overline{[\tilde{f},\tilde{g}]} \ . \tag{27}$$

The shear-Alfvén law, Eq. (9) and the pressure equation (20) are now separated into resonant and non-resonant parts. The helical average of these equations is

$$\frac{\partial \overline{U}}{\partial \tau} + [\overline{\varphi},\overline{U}] + \overline{[\tilde{\varphi},\tilde{U}]} = [\overline{X},\overline{J}] + \overline{[\tilde{X},\tilde{J}]} - \overline{[x,\tilde{p}]} \ , \tag{28}$$

$$[\overline{X},\overline{p}] + \overline{[\tilde{X},\tilde{p}]} = 0 \ . \tag{29}$$

The relative magnitude of the resonant terms is as follows:

(i) $\overline{p} \sim \overline{X} \sim \delta$, $\overline{J} = 2 + O(\delta)$.

(ii) From the η-averaged Ohm's law, Eq. (11), one finds $\overline{\varphi} \sim \frac{\partial}{\partial \tau} \sim \delta$.

The non-resonant quantities are determined by the η-fluctuating part of the equations. For the pressure law, subtracting Eq. (29) from Eq. (20) yields

$$\frac{\partial \tilde{p}}{\partial \eta} = [\tilde{X},\overline{p}] + [\overline{X},\tilde{p}] + [\tilde{X},\tilde{p}] - \overline{[\tilde{X},\tilde{p}]} \ . \tag{30}$$

It follows that $\tilde{p} \sim \delta^2$. $\tilde{p}$ is thus determined to leading order by

$$\frac{\partial \tilde{p}}{\partial \eta} = [\tilde{X},\overline{p}] \ . \tag{31}$$

Thus the non-resonant pressure results from advection of the resonant pressure by the non-helical component of the magnetic field.

From the non-resonant part of Ohm's law, one finds $\tilde{\varphi} \sim \frac{\partial \tilde{X}}{\partial \tau} \sim \delta^2$. This implies that the kinetic terms can be neglected entirely from the non-resonant shear-Alfvén law. The remaining terms are

$$\begin{aligned} \frac{\partial \tilde{J}}{\partial \eta} &= [\tilde{X},\overline{J}] + [\overline{X},\tilde{J}] + [\tilde{X},\tilde{J}] - \overline{[\tilde{X},\tilde{J}]} \\ &\quad - [x,\overline{p}] - [x,\tilde{p}] + \overline{[x,\tilde{p}]} \ . \end{aligned} \tag{32}$$

The leading order term on the right-hand side is $[x, \overline{p}] \sim \delta$, so that $\widetilde{J} \sim \widetilde{X} \sim \delta$. The other terms are then of higher order and Eq. (32) becomes

$$\frac{\partial \widetilde{J}}{\partial \eta} = -[x, \overline{p}] \; . \tag{33}$$

The current $\widetilde{J}$ may be interpreted as a Pfirsch-Schlüter current.[12]

The non-resonant equations can be integrated:

$$\widetilde{p} \;=\; \left[\int d\eta \widetilde{X}, \overline{p}\right] \; , \tag{34a}$$

$$\widetilde{J} \;=-\; \left[\int d\eta \, x, \overline{p}\right] \; . \tag{34b}$$

Substituting the result into Eq. (29) and neglecting the higher order term $\overline{[\widetilde{\varphi}, \widetilde{U}]}$, one finds

$$\frac{\partial \overline{U}}{\partial \tau} + [\overline{\varphi}, \overline{U}] - [\overline{X}, \overline{J}] = -\frac{1}{2\pi} \oint \left\{ \left[x, \left[\int d\eta \widetilde{X}, \overline{p}\right]\right] + \left[\widetilde{X}, \left[\int d\eta \, x, \overline{p}\right]\right] \right\} d\eta \; . \tag{35}$$

Integrating the last term by parts and using Jacobi's identity yields the η-averaged shear-Alfvén law

$$\frac{\partial \overline{U}}{\partial \tau} \;+\; [\overline{\varphi}, \overline{U}] - [\overline{X}, \overline{J}] - [\overline{p}, h] = 0 \; , \tag{36}$$

where

$$h \;=\; \overline{[x, \int d\eta \, \widetilde{X}]} \; . \tag{37}$$

This term may be interpreted as follows:

The curvature in RMHD is given by $\boldsymbol{\kappa} = -\boldsymbol{\nabla} x$. The function x plays a role analogous to gravitational potential in a gravity-driven interchange. It can be shown that, to required order, h is the average of x along a magnetic field line,

$$h = \oint \frac{d\ell}{B} \cdot x \; . \tag{38}$$

Note that only the non-resonant part of the flux contributes at this order, and that the field lines generated by $\widetilde{X}$ alone close after one period. ∇h therefore plays the role of an average curvature in Eq. (36).

B. Calculation of the average curvature

The average curvature is calculated by integrating Ampere's law for the non-resonant current given in Eq. (34b) and substituting the result in Eq. (37). The solution depends of course on the choice of boundary conditions. We are primarily interested in equilibria consisting of two regions (Fig. 2):

(i) A central, low-shear region where the quasi-interchange ordering is satisfied with $q_s = 1$.

(ii) A sheared outer region where $\nabla_{\|} \sim 1$, $p \sim \delta$. The appropriate boundary conditions are then obtained by requiring the solutions in the low-shear region to asymptotically match those in the outer, sheared region.

The integrations are most easily accomplished after Fourier decomposition of the fields:

$$\bar{p}(r,\alpha) = \sum_{n=-\infty}^{+\infty} \bar{p}_n(r) e^{in\alpha} , \tag{39}$$

$$x = \frac{1}{2}\, r \left\{ e^{i(\alpha+\eta)} + e^{-i(\alpha+\eta)} \right\} . \tag{40}$$

The reality condition can be written

$$\bar{p}_n^* = \bar{p}_{-n} . \tag{41}$$

Substituting these expressions into Eq. (35b) one finds

$$\widetilde{X}(r,\alpha,\eta) = \sum_{\pm} \sum_{n=-\infty}^{+\infty} \widetilde{X}_{n,\pm}(r) \exp\left\{ i(n\pm 1)\alpha \pm i\eta \right\} , \tag{42}$$

where the $\widetilde{X}_{n,\pm}(r)$ are determined by

$$\left\{ \frac{1}{r}\frac{d}{dr}\left(r\frac{d}{dr} \right) - \frac{1}{r^2}(n\pm 1)^2 \right\} \widetilde{X}_{n,\pm}(r) = \frac{1}{2r}\left\{ r\frac{d}{dr} \mp n \right\} \bar{p}_n(r) . \tag{43}$$

The general solution regular on axis is

$$\widetilde{\chi}_{n,\pm}(r) = \frac{1}{2}\, r^{-(1\pm n)} \int_0^r r^{1\pm n} \widetilde{p}_n(r) dr + \frac{1}{2}\, \frac{C_{n,\pm}}{(n \pm 1)}\, r^{n\pm 1} \; , \tag{44}$$

where the last term is the solution to the homogeneous equation. This term represents the deformation of the field lines caused by non-resonant currents outside of the low-shear interchange region. These currents are themselves induced by the perturbations inside this region. The constants $C_{n,\pm}$ are determined by asymptotically matching the inside solution, Eq. (44), to the solution in the outer region.

We now consider the equations in the outer region. The shear-Alfvén law is given to required order by

$$\frac{\partial \widetilde{J}}{\partial \eta} = [\widetilde{\chi}, \overline{J}] + [\overline{\chi}, \widetilde{J}] + [x, \widetilde{p}] \; . \tag{45}$$

Of course the η-averaged components of the fields are no longer resonant. The line-bending forces and circular confinement vessel then combine to constrain the fields so that all the η-averaged components except $n = 0$ vanish as the shear becomes large. Thus, for $n \neq 0$ the shear-Alfvén law becomes

$$\frac{\partial \widetilde{J}}{\partial \eta} = [\chi_0, \widetilde{J}] + [\widetilde{\chi}, J_0] \; , \tag{46}$$

where χ_0 and J_0 are the $n = 0$ components of $\overline{\chi}$ and $\overline{J}$, respectively. As the low-shear region is approached, $\chi_0 \rightarrow o(\delta)$ and the solutions to this equation take the asymptotic form

$$\widetilde{\chi}_{n,\pm} \sim A_{n,\pm}\, r^{-(n\pm 1)} + B_{n,\pm}\, r^{(n\pm 1)} \; . \tag{47}$$

Note that Eq. (46) is linear in $\widetilde{\chi}$, so that only the ratio $\sigma_{n,\pm} = A_{n,\pm}/B_{n,\pm}$ is relevant. The constants $\sigma_{n,\pm}$ are determined by integrating Eq. (46) inwards starting from the vessel wall or from the appropriate mode-rational surface.

Returning to the low-shear solution, one finds that the integrand in Eq. (44) will vanish as the shear increases in the matching region. It follows that the asymptotic form of the inner solution in the outer region is

$$\chi_{n,\pm} \sim \left(\frac{1}{2}\int_0^1 r^{1\pm n}\bar{p}_n(r)dr\right)\cdot r^{-(1\pm n)} + \left(\frac{1}{2}\,\frac{C_{n,\pm}}{(n\pm 1)}\right)\cdot r^{n\pm 1}\ , \tag{48}$$

where the upper limit of integration has been taken to be the confinement vessel wall. The matching of the solutions is thus achieved when

$$\sigma_{n,\pm} = \frac{n\pm 1}{C_{n,\pm}}\int_0^1 r^{1\pm n}\,\bar{p}_n(r)dr \qquad , \qquad n\neq 0\ . \tag{49}$$

The effect of the currents induced in the outer region is thus entirely contained in the constants σ. Note that effects related to the motion of the matching region are of higher order in δ.

The potential function h is now found by substituting Eq. (44) into Eq. (37). We find

$$h \;=\; \frac{1}{2}\,\bar{p}+\lambda\ , \tag{50}$$

where

$$\lambda \;=\; \sum_{n=-\infty}^{+\infty}\lambda_n e^{in\alpha}\ , \tag{51}$$

$$\lambda_n \;=\; \frac{1}{2}\,C_{n,+}r^n\ . \tag{52}$$

The terms containing $C_{n,-}$, corresponding to perturbations with pitch $d\theta/d\zeta$ less than one, do not contribute. This is not a local effect: it is a consequence of requiring the perturbation to be regular at the origin.

The result of the curvature calculation may now be substituted in the η-averaged shear-Alfvén law. The resulting, interchange-reduced shear-Alfvén law takes the form

$$\frac{\partial\overline{U}}{\partial\tau}+[\overline{\varphi},\overline{U}]-[\overline{\chi},\overline{J}]-[\overline{p},\lambda]=0\ . \tag{53a}$$

This equation is completed by

$$[\overline{\chi},\overline{p}]=0\ , \tag{53b}$$

and the matching condition

$$C_n\sigma_n = (n+1)\int_0^1 r^{n+1}\,\bar{p}_n(r)dr \ , \tag{53c}$$

where $\sigma_n = \sigma_{n,+}$. Equation (53b) is obtained from Eq. (29) by neglecting the higher-order term $\overline{[\tilde{X},\tilde{p}]}$.

The dimensionality of the problem has thus been reduced to two. It should be emphasized, however, that the plasma does not have helical symmetry. Significantly, the interchange is found to be driven only by the part of the curvature which is caused by the currents induced in the sheared outer region.

We conclude this section by considering the η-averaged Ohm's law:

$$\frac{\partial \overline{X}}{\partial \tau} + [\overline{\varphi},\overline{X}] + \overline{[\tilde{\varphi},\tilde{X}]} = 0 \ . \tag{54}$$

The last term may be neglected. It follows that, to the order of the calculation, $\overline{X}$ is an advected quantity and the quantity

$$T = \int S(\overline{X}) r dr d\alpha \tag{55}$$

is conserved by the interchange-reduced system for any choice of the function S.

IV. Equilibrium Bifurcation

The equations derived in the preceding section are now applied to the nonlinear evolution of the quasi-interchange mode. This is accomplished through a perturbation expansion in the mode amplitude ξ, where ξ is the displacement of the flux surfaces from their equilibrium position. From Eq. (1), the nonlinear regime near marginal stability is found to be characterized by $\gamma \sim \frac{d}{d\tau} \sim \xi \ll 1$.

The following two basic assumptions are made:

(i) The perturbed initial state is taken to be accessible from the equilibrium within the confines of perfect conductivity theory.[8] That is, the integral invariants given by Eqs. (18)

and (55) take the same value for the perturbed initial state as for the equilibrium state. A similar restriction on the initial conditions has already been used to replace Eq. (12) by Eq. (20).

(ii) The mode is assumed to grow coherently. More specifically, the near-marginal eigenvalue is assumed to be simple, with $\gamma \ll \omega$ where ω is the eigenfrequency of the nearest nonlinearly driven mode.

In the following the equilibrium quantities will be denoted by the subscript e.

The accessibility constraint requires

$$C = \int F(p_e) dV = \int F(p) dV \ , \tag{56}$$

for any choice of F. To order ξ^3, this condition is equivalent to

$$\bar{p}_0(r) = p_e(r) + \frac{1}{r}\frac{d}{dr}\left(\frac{r}{p'_e}\, p_1^2\right) \ , \tag{57}$$

where $p'_e = \frac{dp_e}{dr}$. Henceforth, the overbars will be omitted. The flux conservation constraint, Eq. (55), requires similarly

$$\chi_0(r) \ = \ \chi_e(r) + \frac{1}{r}\frac{d}{dr}\left(\frac{r}{\chi'_e}\, \chi_1^2\right) \ . \tag{58}$$

Note that

$$\chi'_e(r) \ = \ \left(1 - \frac{1}{q(r)}\right) \cdot r \ , \tag{59}$$

where $q(r)$ is the rotational transform, correct to first order, of the flux surface which reduces to a circle of radius r to lowest order in δ.

We now consider the interchange-reduced shear-Alfvén and pressure laws, Eq. (53). To first order in ξ they can be written

$$\chi'_e J_1 - J'_e \chi_1 \ = \ -p'_e \lambda_1 \ , \tag{60a}$$

$$\chi'_e p_1 - p'_e \chi_1 \ = \ 0 \ . \tag{60b}$$

The quantities φ and U can be shown from Ohm's law to be of order ξ^2, so that the term $\frac{\partial U}{\partial \tau}$ appears only in the third-order equations, while $[\varphi, U]$ is of even higher order and is neglected in the following treatment.

In terms of the convenient abbreviation

$$\dot{F} = \frac{F'}{\chi_e'} = \frac{dF_e}{d\chi_e} , \tag{61}$$

Eq. (60) becomes

$$J_1 - \dot{J}_e \chi_1 = -\dot{p}_e \lambda_1 , \tag{62a}$$

$$p_1 = \dot{p}_e \chi_1 . \tag{62b}$$

The left-hand side of Eq. (62a) contains a second-order differential operator applied to χ_1. This operator can be inverted for an arbitrary source function $f(r)$. Let

$$\chi_1(r) = \chi_e' \xi_1(r) . \tag{63}$$

$\xi_1(r)$ is the $n = 1$ component of the displacement of the flux surface. Substituting Eq. (63) into the left-hand side of Eq. (62a), and replacing the right-hand side by the arbitrary source $f(r)$, one finds

$$J_1 - \dot{J}_e \chi_1 = \frac{1}{r\chi_e'} \frac{d}{dr} \left(r(\chi_e')^2 \frac{d\xi_1}{dr} \right) = f(r) . \tag{64}$$

Integrating twice yields

$$\xi_1(r) = -\int_r^1 \frac{d\hat{\rho}}{\hat{\rho}(\chi_e'(\hat{\rho}))^2} \int_0^{\hat{\rho}} f(\rho)\chi_e'(\rho)\rho d\rho . \tag{65}$$

The solution to Eq. (62a) is now found by replacing f by $-\dot{p}_e\lambda_1$, in Eq. (65). p_1, given by Eq. (62b) can then be substituted into the matching condition. After integration by parts, this becomes

$$\sigma_1 = \int_0^1 \frac{(\delta \cdot \hat{\beta}_p)^2}{\left(\frac{1}{q} - 1\right)^2} r^5 dr , \tag{66a}$$

where $\hat{\beta}_p$ is the RMHD normalized poloidal beta,

$$\delta \cdot \hat{\beta}_p = -\frac{1}{r^4} \int_0^r \rho^2 p_e'(\rho) d\rho \ . \tag{66b}$$

Equation (66) is of course the linear marginal stability condition for the $n = 1$ mode. Note that this equation is in complete agreement with the full MHD result of Refs. 5 and 6.

To next order in ξ, the $n = 1$ mode couples into $n = 0$ and $n = 2$. The $n = 0$ components have already been calculated from the conservation laws: they are given by Eqs. (57) and (58). The $n = 2$ components are determined by Eq. (53):

$$J_2 - \dot{J}_e \chi_2 = -\dot{p}_e \lambda_2 + \frac{1}{2} \ddot{J}_e \chi_1^2 - \ddot{p}_e \chi_1 \lambda_1 \ , \tag{67a}$$

$$p_2 = \dot{p}_e \chi_2 + \frac{1}{2} \ddot{p}_e \chi_1^2 \ . \tag{67b}$$

Equation (67a) is a second-order inhomogeneous differential equation for χ_2. Unlike Eq. (62a) for χ_1, however, it cannot be integrated by simple quadratures. Assuming nonetheless that a solution has been found, the constant C_2 is then determined by the matching condition:

$$C_2 \sigma_2 = 3 \int_0^1 r^3 p_2(r) dr \ . \tag{68}$$

The third-order corrections to the $n = 1$ equations can now be calculated. The corrected source term f becomes

$$\begin{aligned} f = & -\dot{p}_e \lambda_1 - \ddot{p}_e \left((\chi_2 + \chi_0 - \chi_e) \lambda_1 + \chi_1 \lambda_2 \right) + \ddot{J}_e \chi_1 \chi_2 \\ & - \dot{J}_e \chi_1 \dot{\chi}_0 + \chi_1 \dot{J}_0 - \frac{1}{2} \dddot{J}_e \chi_1^3 - 2 \ddot{J}_e \chi_1^2 \dot{\chi}_1 \\ & + \frac{1}{2} \dddot{p}_e \lambda_1 \chi_1^2 + 2 \ddot{p}_e \chi_1 \dot{\chi}_1 \lambda_1 + 2 \ddot{p}_e \dot{\lambda}_1 \chi_1^2 - \frac{1}{r \chi_e'} \frac{d}{dr} \left(r^3 \frac{d}{dr} \left(\frac{\partial^2 \xi_1}{\partial \tau^2} \right) \right) \ . \end{aligned} \tag{69}$$

The corrected pressure fluctuation is

$$p_1 = \dot{p}_e \chi_1 + \ddot{p}_e (\chi_1 \chi_2 + \chi_1 \chi_0) + \frac{1}{2} \dddot{p}_e \chi_1^3 \ .$$

Replacing these quantities in the matching condition yields the bifurcation equation, Eq. (1).

It is clear from this analysis that the practical calculation of the nonlinear corrections can only be accomplished for special equilibria such that Eq. (67a) can be inverted analytically. The solution of the bifurcation equations for model profiles is the subject of the following section.

V. Solution for Model Profiles

A. Constant current case

It is assumed throughout this section that the pressure profile is parabolic in the low-shear region: $p_e' = -2p_0 r$.

We consider first a safety-factor profile with constant $q(r) = q_0$ for $r < r_s$ and with q rising abruptly beyond r_s. This requires a thin current-sheet at $r = r_s$ and a constant current profile within $r < r_s$. Such configurations have the property that the equilibrium fields are linearly related in the constant-current, parabolic pressure region: that is, $\dot{p}_e =$ cst. and $\dot{J}_e = 0$. The only remaining nonlinear coupling arises from the flux and pressure-conservation constraints, which imply coupling to the $n = 0$ component only. This case is thus of a quasilinear nature.

The bifurcation equation is obtained by following the procedure described in the preceding section. The linear eigenmode is given by

$$\chi_1(r) = -\frac{\kappa_0 C_1}{8} r^3 + A \cdot r \quad , \quad r < (r_s - w) \ , \tag{70}$$

where

$$\kappa_0 = \frac{p_0}{\left(\frac{1}{q_0} - 1\right)} \ , \tag{71}$$

and w is the half-width of the current sheet. For $w \ll 1$, the integration constant A is determined by the condition $\chi_1(r_s) = 0$. The third-order accurate flux perturbation is then

$$\chi_1 = \frac{\kappa_0}{8}\, r \cdot (r_s^2 - r^2) \left(C_1 - \left(\frac{1}{q_0} - 1\right)^{-2} \frac{d^2 C_1}{dt^2} \right)$$

$$- \left(\frac{\kappa_0 C_1}{4}\right)^3 \cdot \left(\frac{1}{q_0} - 1\right)^{-2} \left(r^4 - 3r_s^2 r^2 + 2r_s^4\right) r \,. \tag{72}$$

The matching condition yields the bifurcation equation:

$$\frac{d^2 \widehat{\xi}}{d\tau^2} = \left(\frac{r_s^6}{24\sigma_1}\, p_0^2 - \left(\frac{1}{q_0} - 1\right)^2 \right) \widehat{\xi} - 12 \left(\frac{1}{q_0} - 1\right)^2 \widehat{\xi}^3 \,, \tag{73}$$

where $\widehat{\xi} = \xi_1(0)/r_s$. This is thus a supercritical bifurcation. Note that this result is independent of the precise form of the current profile in the outer region, since σ_1 does not appear in Γ.

B. Gaussian rotational transform

Before drawing conclusions, it is desirable to solve the bifurcation equations for a fully nonlinear case. The following q-profiles satisfy this requirement while remaining analytically tractable. Let

$$\left(\frac{1}{q} - 1\right) = \left(\frac{1}{q_0} - 1\right) \exp\left(\frac{r^2}{2s^2}\right) \,, \tag{74}$$

with $s^2 = \frac{1}{2}(r_2)^2 \left|\ell n \left[2 \cdot (1 - 1/q_0)\right]\right|^{-1} < 1$, where r_2 is the radius of the $q = 2$ surface. In terms of the radial variable z defined by $z = r^2/s^2$, the equilibrium quantities are given by

$$\dot{p}_e = 2\kappa_0\, e^{-z/2} \,, \tag{75a}$$

$$\dot{J}_e = (4 + z)/s^2 \,. \tag{75b}$$

The solution of the linear equations is

$$\chi_1 = K_1 z^{1/2}\, e^{-z/2} \,, \tag{76}$$

where $K_1 = \kappa_0 C_1 s^3/8$. The marginal stability condition is

$$\kappa_{0,c}^2 = 4\sigma_1/s^6 + O(\xi^2) . \tag{77}$$

The equation for the $n = 2$ flux-perturbation χ_2 is

$$\hat{J}_2 \quad - \quad (4+z)\chi_2 = -s^4 \kappa_0 C_2 z \; e^{-z/2} - \frac{9K_1^2}{\left(\frac{1}{q_0} - 1\right)} - \frac{z}{s^2} \; e^{-3z/2} , \tag{78}$$

where

$$\hat{J}_2 \quad = \quad 4\left(z\frac{d^2\chi_2}{dz^2} + \frac{d\chi_2}{dz} - \frac{1}{z}\,\chi_2\right) . \tag{79}$$

An integral representation of the solution to this equation can be found by the method of kernels.[13]

$$\chi_2 = \left\{\frac{\kappa_0 C_2 s^4}{10} + \frac{9\sqrt{2}}{8s^2}\,\frac{K_1^2}{\left(\frac{1}{q_0}-1\right)} \int_0^1 \; e^{-2y} y^{3/2}(1+y)^{-1/2} dy\right\} z e^{-z/2} . \tag{80}$$

The constant C_2 is determined by the matching conditions. One finds

$$C_2 = \frac{21}{20}\,\frac{\kappa_0 s^2 K_1^2}{\left(\frac{1}{q_0}-1\right)}\,\frac{1}{\left(\sigma_2 - \frac{3}{5}s^8\kappa_0^2\right)} . \tag{81}$$

Note that $C_2 \to \infty$ for $\sigma_2 = \frac{3}{5}s^8\kappa_0^2$. This is of course the linear marginal stability condition for the $n = 2$ mode. Comparing this to the marginal stability condition for the $n = 1$ mode, $\sigma_1 = \frac{s^6}{4}\,\kappa_0^2$, one concludes that degeneracy occurs when $\sigma_2/\sigma_1 = 2.4s^2$. Numerical and analytical estimates indicate that typically $\sigma_2/\sigma_1 \gtrsim 4s^2$ so that the non-degeneracy assumption is well satisfied.

Placing these results in the $n = 1$ matching condition yields the bifurcation equation:

$$\frac{d^2\xi}{d\tau^2} \quad = \quad 8\left(\frac{s^6}{4\sigma_1}\,p_0^2 - \left(\frac{1}{q_0} - 1\right)^2\right)\xi + \Gamma\xi^3 , \tag{82}$$

where

$$\Gamma \quad \cong \quad -\frac{5.39}{s^4}\left(\frac{\sigma_2 - 2.95\sigma_1 s^2}{\sigma_2 - 2.4\sigma_1 s^2}\right)\left(\frac{1}{q_0} - 1\right)^2 . \tag{83}$$

Thus $\Gamma < 0$ for $\sigma_2/\sigma_1 > 2.95s^2$. It is noteworthy that $|\Gamma|$ decreases as the marginal stability threshold of the $n = 2$ mode approaches that of the $n = 1$ mode. This is also the case for the free-boundary kink bifurcation (Fig. 3).[7] However, exterior current profiles with $\sigma_2/\sigma_1 < 2.95s^2$ were not found in this investigation. We must therefore conclude that the fully nonlinear gaussian-profile case is also supercritical.

VI. Discussion

The saturation of the growth of the $n = 1$ quasi-interchange is related to the existence of nearby bifurcated equilibria. The eigenmode expansion approach used in this investigation guarantees the stability of these secondary equilibria to low mode-number interchange-like perturbations. However, these equilibria may be unstable to large mode-number ballooning instabilities. Such a two-instability mechanism has been suggested by Bussac et al. for rotational transform profiles with an off-axis minimum.[14] Note that the lack of symmetry of the bifurcated equilibria implies the existence of small regions of magnetic stochasticity. It is unlikely, however, that this effect can account for the sudden onset of growth during sawtooth disruptions.

Another possibility is that the quasi-interchange is stabilized by kinetic effects until sufficient free energy has been accumulated to account for the large growth-rates observed. Kinetic effects on linear stability have been considered by Hastie and Hender.[5]

Acknowledgments

The author is grateful to R.D. Hazeltine for encouragement and many helpful suggestions, and to Jim Meiss and A.Y. Aydemir for useful discussions.

References

1. A.W. Edwards, D.J. Campbell, W.W. Engelhardt, H.V. Fahrbach, R.D. Gill, R.S. Granetz, S. Tsuji, B.J.D. Tubbing, A. Weller, J. Wesson, and D. Zasche, Phys. Rev. Lett. **57**, 210 (1986).

2. J.A. Wesson, Plasma Physics and Controlled Fusion **28**, 243 (1986).

3. J.A. Wesson, P. Kirby, and M.F.F. Nave, in *Plasma Physics and Controlled Nuclear Fusion Research 1986*, Kyoto, Japan, 1986 (IAEA, Vienna, 1987), Vol. 2, p. 3.

4. A.Y.A. Aydemir. Phys. Rev. Lett. **59**, 649 (1987).

5. R.J. Hastie, T.C. Hender, Nucl. Fusion **28**, 585 (1988).

6. F.L. Waelbroeck, R.D. Hazeltine, Phys. Fluids **31**, 1217 (1988).

7. P.H. Rutherford, H.P. Furth, M.N. Rosenbluth, in *Plasma Physics and Controlled Nuclear Fusion Research* (International Atomic Energy Agency, Vienna, 1971), Vol. 1, p. 533.

8. M.N. Rosenbluth, R.Y. Dagazian, and P.H. Rutherford, Phys. Fluids **16**, 1894 (1973).

9. H.R. Strauss, Phys. Fluids **20**, 1354 (1977).

10. A.A. Ware and F.A. Haas, Phys. Fluids **9**, 956 (1966).

11. P.J. Morrison and R.D. Hazeltine, Phys. Fluids **27**, 886 (1984).

12. M. Kotschenreuther, R.D. Hazeltine and P.J. Morrison, Phys. Fluids **28**, 294 (1985).

13. E.L. Ince, *Ordinary Differential Equations,* (Dover, New York, 1956).

14. M.N. Bussac and R. Pellat, private communication.

Figure Captions

1. Bifurcations of equilibrium. Solid lines indicate stable equilibria, dashed lines unstable equilibria. (a) Supercritical bifurcation. (b) Subcritical bifurcation.

2. Equilibrium q-profile.

3. Effect of near-degenerescence on bifurcated equilibria.

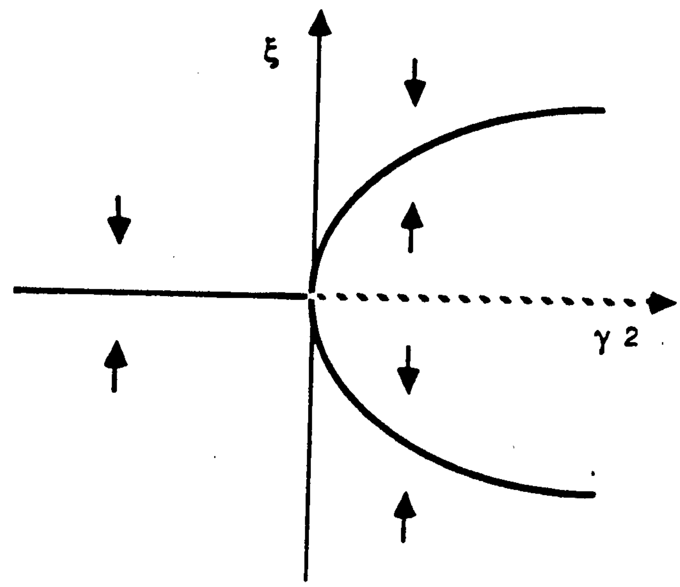

Fig. 1(a)

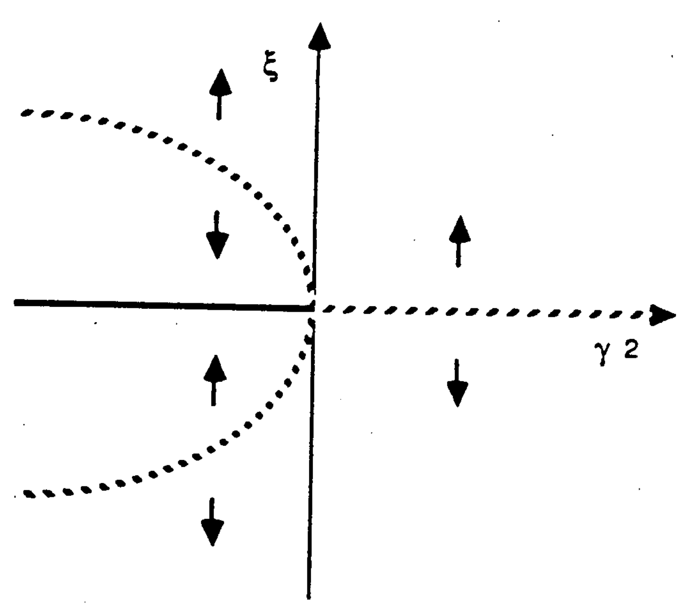

Fig. 1(b)

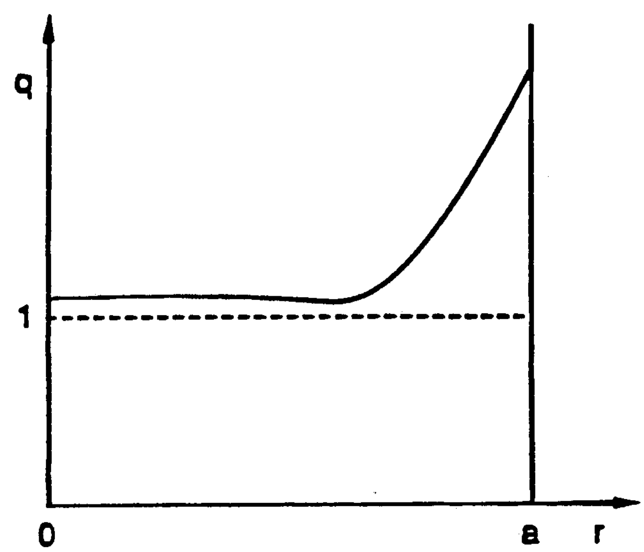

Fig. 2

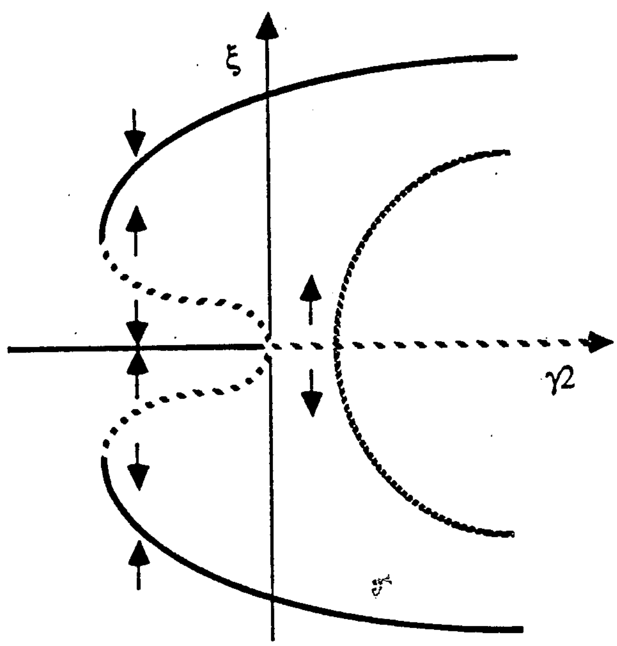

Fig. 3